Mon. Not. R. Astron. Soc. **395,** 1135–1145 (2009) doi:10.1111/j.1365-2966.2009.14621.x

Galaxy clusters in the line of sight to background quasars – II. Environmental effects on the sizes of baryonic halo sizes

Nelson Padilla,[1⋆] Ivan Lacerna,[1] Sebastián Lopez,[2] L. Felipe Barrientos,[1] Paulina Lira,[2] Heather Andrews[1] and Nicolás Tejos[2]

[1]*Departamento de Astronomía y Astrofísica, Pontificia Universidad Católica de Chile, Santiago, Chile*
[2]*Departamento de Astronomía, Universidad de Chile, Casilla 36-D, Santiago, Chile*

Accepted 2009 February 10. Received 2009 February 9; in original form 2008 November 3

ABSTRACT

Based on recent results on the frequency of Mg II absorption-line systems in the spectra of QSO behind RCS clusters (QbC), we analyse the effects of the cluster environment on the sizes of baryonic haloes around galaxies. We use two independent models: (i) an empirical halo occupation model which fits current measurements of the clustering and luminosity function of galaxies at low and high redshifts and (ii) the GALFORM semi-analytic model of galaxy formation, which follows the evolution of the galaxy population from first principles, adjusted to match the statistics of low- and high-redshift galaxies. In both models, we constrain the Mg II halo sizes of field and cluster galaxies using observational results on the observed Mg II statistics. Our results for the field are in good agreement with previous works, indicating a typical Mg II halo size of $r_{\rm Mg\,II} \simeq 50\,h_{71}^{-1}$ kpc in the semi-analytic model, and slightly lower in the halo occupation number approach. For the cluster environment, we find that both models require a median Mg II halo size of $r_{\rm Mg\,II} < 10\,h_{71}^{-1}$ kpc in order to reproduce the observed statistics on absorption-line systems in clusters of galaxies. Based on the Chen & Tinker (2008) result that stronger systems occur closer to the Mg II halo centre, we find that strong absorption systems in clusters of galaxies occur at roughly a fixed fraction of the cold-warm halo size out to $1\,h_{71}^{-1}$ Mpc from the cluster centres. In contrast, weaker absorption systems appear to occur at progressively shorter relative fractions of this halo as the distance to the cluster centre decreases. These results reinforce our conclusions from Lopez et al. and provide additional independent support for the stripping scenario of the cold gas of galaxies in massive clusters by the hot intracluster gas, e.g. as seen from X-ray data.

Key words: galaxies: clusters: general – galaxies: haloes – galaxies: structure.

1 INTRODUCTION

Understanding the influence of environment on galaxy evolution in either the field or galaxy clusters, provides important missing clues on the interplay of internal and external mechanisms that shape the galaxy population. In this work, we concentrate on the statistics of Mg II absorption systems in galaxies associated with high-redshift clusters, as recently obtained by Lopez et al. (2008, hereafter Paper I). Our aim is to confront those statistics with different galaxy models in order to constrain the sizes of the cold-warm baryonic component of cluster galaxies.[1]

Ever since the first studies of quasi-stellar object (QSO) absorption lines, Mg II was recognized as an excellent tracer of high-redshift galaxies (Bergeron & Stasinska 1986; Lanzetta, Turnshek & Wolfe 1987; Tytler et al. 1987; Petitjean & Bergeron 1990; Steidel & Sargent 1992; Churchill et al. 2000). These seminal works were then followed by numerous studies (Churchill et al. 1999; Nestor, Turnshek & Rao 2005; Lynch, Charlton & Kim 2006; Nestor, Turnshek & Rao 2006; Prochter, Prochaska & Burles 2006; Narayanan et al. 2007) that were able to distinguish between weak and strong Mg II absorption systems as possibly two distinct populations. When selecting the stronger Mg II systems (with rest-frame equivalent width (EW) $W_0^{2796} > 0.3$ Å), the associated galaxies present a slight preference for blue, starburst galaxies with high metallicities (Ellison, Kewley & Mallén-Ornelas 2005; Zibetti et al. 2007). However, it is still not clear whether the stronger systems really occur in extended (hundreds of kpc) and virialized haloes already in place at $z = 2$ (Churchill, Kacprzak & Steidel 2005; Steidel et al. 2002) or if some

⋆E-mail: npadilla@astro.puc.cl

[1] The temperature of the Mg II gas is expected to be a few 10^4 K, and therefore is termed here cold-warm gas. Note that in some other cases, e.g. in Chen & Tinker (2008), Mg II is referred to as cold gas.

are the signature of violent galaxy-scale outflows (Bouche et al. 2006; Prochter et al. 2006).

Despite these extensive absorber-galaxy studies, and perhaps due to our lack of knowledge about the nature of Mg II absorbers, it has been difficult so far to establish correlations between absorption-line strength and absorber-galaxy luminosity and impact parameter. Although some tentative correlations were found in the past (Steidel et al. 1995; Churchill et al. 1999), it is now becoming clear from deep imaging of the QSO fields that not only the Mg II covering fraction must be less than unity (Chen & Tinker 2008; Kacprzak et al. 2008), contrary to what was assumed for years, but also there must be correlations with the galaxy environment.

In Paper I, we proposed to study the environmental dependence of the size of the cold-warm baryonic component using the frequency of Mg II in the line of sight (LOS) to QSOs close in projection to foreground clusters. Thus, contrary to previous studies, our samples were constructed in an unbiased way by selecting a set of known galaxy overdensities and then searching for absorption systems in their neighbourhoods. In these particular LOS, we obtained a comparatively flatter EW distribution with respect to what has been obtained for the field. This result suggests that the cluster environment could be pruning the baryonic halo size significantly.

Generally, the interpretation of the statistics on Mg II absorption systems in the field[2] has been done following analytic approaches (as in Churchill et al. 1999). Only more recent works (Chen & Tinker 2008; Tinker & Chen 2008) use a model motivated by observational data within a cosmological framework, the halo occupation model (HO model, Seljak 2000; Scoccimarro et al. 2001; Berlind & Weinberg 2002; see Zheng & Weinberg 2007, and references therein), to study the origin of the Mg II absorption systems, their geometry and the dependence of EW with the distance from a Mg II halo centre.[3]

Building upon the results presented in Paper I, we perform a theoretical study of Mg II absorption systems using models to determine how the size of the cold-warm baryonic halo depends on environment. In order to do this, we use two different models, (i) a HO model, constructed empirically by Cooray (2006), adopting a Λ cold dark matter (ΛCDM) cosmology and (ii) a semi-analytic model by Bower et al. (2006, a version of the GALFORM model by Cole et al. 2000) which follows the evolution of galaxies in a ΛCDM universe from first principles, tuned to reproduce the observed galaxy population at a wide range of redshifts (other semi-analytic models include Baugh et al. 2005, Croton et al. 2006 and Lagos, Cora & Padilla 2008, among others). We then concentrate on determining the cold-warm baryonic halo sizes and their dependence on galaxy environment, without modelling the distribution of gas in a direct way, but instead establishing the required cold-warm halo size needed to reproduce the observed Mg II absorber statistics presented in Paper I for clusters of galaxies. For simplicity, we start assuming a unity-covering fraction and then discuss the implications of this choice.

Throughout this paper, the cosmological model adopted is characterized by the 'concordance' parameters in line with estimates from the large-scale distribution of galaxies and the temperature fluctuations in the cosmic microwave background (Sánchez et al. 2006), namely, $\Omega_{\rm m} = 0.25$, $\Omega_\Lambda = 0.75$, $\Omega_{\rm b} = 0.045$, a Hubble constant $H_0 = 71 \times h_{71}$ km s^{-1} Mpc^{-1}, with $h_{71} = 1$, $n = 1$ and $\sigma_8 = 0.9$.

The paper is organized as follows. In Section 2, we briefly review the observational results from Paper I and the additional refinements applied to them to take into account the contamination from the field and the large-scale structure. Section 3 presents the two models in detail. Section 4 describes the results, and a discussion is presented in Section 5. Our conclusions are summarized in Section 6.

2 OBSERVATIONS

In this section, we describe the available data sets used for this work and the corrections we have made to account for contamination from the field and large-scale structures.

2.1 The data

In Paper I, we used the Red-sequence Cluster Survey (RCS, Gladders & Yee 2005) to perform a search of clusters in the LOS to background quasars, and constructed two different sets of cluster–QSO pairs. The first set includes 46 high-resolution QSO spectra, and the second comprises lower resolution spectra (these numbers do not include restrictions on signal-to-noise ratios). In all cases, the maximum physical distance between the LOS to QSOs and the cluster centres was set to $2\,h_{71}^{-1}$ Mpc, for a total sample of 529 cluster–QSO pairs.

We estimate the median mass of RCS clusters in the sample using the $B_{\rm gcR}$ parameter (Gilbank et al. 2007) which can be used to estimate individual cluster masses. For this work, we only take into account results from clusters with at least a 2σ detection of $B_{\rm gcR}$ (i.e. 2σ away from zero). For this subsample of RCS clusters (all of which are paired to a background QSO for a total of 212 pairs), we find a median mass of $(1.64^{+0.856}_{-0.345}) \times 10^{14}\,h_{71}^{-1}\,{\rm M}_\odot$ (errors correspond to the 20 and 80 percentiles of the mass distribution) which we will use in the remainder of this work.

Clusters in the RCS are identified using a likelihood method which fits simultaneously for a projected cluster density profile and a red sequence at different redshifts (see Paper I for more details); this method produces an estimate of the cluster photometric redshift as a by-product. A Mg II system is associated with a RCS cluster when the redshift of the absorption falls within a 1σ interval around the cluster photometric redshift. In some cases, a given absorption system can satisfy this criterion for more than one cluster, in which case we test two different options, to assign the absorption system (i) to the closest cluster in projection (referred to as 'nearest cluster') and (ii) to the farthest cluster in projection ('farthest cluster'). We will show that this choice does not affect our results in a significant way, respectively.

Our subsamples are defined via lower limits of EW. This is particularly important since without a clear modelling of the dependence of the line strength in our models we cannot exclude the occurrence of strong lines, particularly when taking into account indications that these occur closer to the centre of the absorbing galaxy

[2] In this paper, we refer to 'the field' as a collection of objects which has been drawn at random from the full galaxy population, and therefore includes many different environments, from very underdense regions to high-mass clusters. This coincides with the selection of QSOs made by several authors to detect Mg II absorption systems, and will be adopted in our analysis of the numerical models.

[3] The HO models which we refer to in this paper, are rather complex Monte Carlo simulations that reproduce density profiles of haloes of different sizes via fits to numerical simulation results, and populate these haloes with baryonic components following observational measurements of statistics such as the luminosity and correlation functions. All other non-HO models assuming statistical distributions for observational quantities will be referred to simply as Monte Carlo simulations.

(Chen & Tinker 2008). We construct (i) sample weak and strong systems (S:WS) which include all QSO–cluster pairs from the high-resolution spectra and (ii) sample strong systems only (S:St) which consists of QSO–cluster pairs selected from the low-resolution data. Note that sample S:St includes the QSO–cluster pairs from S:WS (all the available pairs), but only considers absorption systems with EW above the lower limit of 1 Å. We define hits in the same fashion as in Paper I, i.e. absorption systems within $\pm\Delta z$ of a cluster redshift, where Δz is the uncertainty in the cluster redshift.

Note that in order to maximize the number of hits, we do not impose the constrains on EW completeness or pair redshifts used in Paper I to correct for cluster completeness. As we show below, these more relaxed sample definitions introduce variations in our results that are negligible when compared to the field and clustering corrections.

2.2 Correcting for systematic effects in the cluster–QSO pair information

The number of hits, $N_{\rm hits}$, varies with the impact parameter to the cluster centre (see Tables 1 and 2). The number of QSO–cluster pairs is larger than the number of QSOs with measured spectra since in many cases there are two or more clusters in the QSO LOS. Given that a Mg II absorption is associated with a cluster only if the redshift difference is within the cluster photometric redshift error, Δz, there is a chance that some of these hits will have actually taken place in the field (which corresponds to the average environment including voids and clusters, statistically) rather than in the associated RCS cluster. Therefore, we make a first correction to the number of hits by setting:

$$N_{\rm hits}^{\rm fc} = N_{\rm hits} - N_{\rm field}, \tag{1}$$

where the correction from the field takes the form

$$N_{\rm field} = \frac{{\rm d}N}{{\rm d}z}(z) \times 2\Delta z, \tag{2}$$

with z being the photometric redshift of the cluster, $2\Delta z$ is summed over all clusters considered in a given sample and ${\rm d}N/{\rm d}z$ is the field estimate from the literature. For S:WS, ${\rm d}N/{\rm d}z$ is given by

$$\frac{{\rm d}N}{{\rm d}z} = 1.9306 + N_*(1+z)^{\alpha} \exp\left[-\frac{W_0}{W_*}(1+z)^{-\beta}\right], \tag{3}$$

where the first term corresponds to the Churchill et al. (1999) estimate extended to $0.015 < W_0^{2796} < 0.3$ Å and the second term corresponds to the Nestor et al. (2005) estimate for absorbers with EWs higher than W_0, which in this case is set to $W_0 = 0.3$ Å; their published parameter values are $N_* = 1.001(\pm0.132)$, $\alpha = 0.226(\pm0.170)$, $W_* = 0.443(\pm0.032)$, $\beta = 0.634(\pm0.097)$ (uncertainties are shown only to illustrate the accuracy of the fit). For sample, S:St ${\rm d}N/{\rm d}z$ is given by the second term with $W_0 = 1$ Å. The adopted redshift corresponds to the median redshift of the RCS cluster sample, median $(z) = 0.6$. The field corrections are listed in column 3 of Tables 1 and 2.

It is well known that clusters occupy biased density peaks in the distribution of matter which are characterized by a high-amplitude cluster-mass cross-correlation function (see e.g. Croft et al. 1997; Padilla et al. 2001). Hence, a correction has to be introduced to take into account the enhanced matter density around clusters which would increase the occurrence of Mg II absorbers from the field in the surrounding few Mpc around each cluster.

We then proceed to calculate the effect of clustering in the region surrounding the clusters, for which we propose a correction of the form

$$N_{\rm hits} = N_{\rm hits}^{\rm fc} - N_{\xi{\rm corr}}, \tag{4}$$

where $N_{\xi{\rm corr}}$ includes the expected excess of field hits due to the overdensity around our cluster sample:

$$N_{\xi{\rm corr}} = I \times N_{\rm field}, \tag{5}$$

where the factor I is calculated using the cluster-mass cross-correlation function as

$$I = \frac{\displaystyle\int_{r_{\rm cm}(z-\Delta z)}^{r_{\rm cm}(z)-Y_{\rm c}} \frac{n(b,\,y')}{\langle n\rangle}{\rm d}y + \int_{r_{\rm cm}(z)+Y_{\rm c}}^{r_{\rm cm}(z+\Delta z)} \frac{n(b,\,y')}{\langle n\rangle}{\rm d}y}{\displaystyle\int_{r_{\rm cm}(z-\Delta z)}^{r_{\rm cm}(z)-Y_{\rm c}} {\rm d}y + \int_{r_{\rm cm}(z)+Y_{\rm c}}^{r_{\rm cm}(z+\Delta z)} {\rm d}y} - 1, \tag{6}$$

where the comoving distance in the redshift path is $Y_{\rm c} = \sqrt{r_{90}^2 - b^2}$, $r_{\rm cm}$ indicates comoving distance, $r_{90} = 1.92\,h_{71}^{-1}$ Mpc is the median of the radius containing 90 per cent of the cluster galaxies for our sample of RCS clusters, $\langle n\rangle$ is the average galaxy density and $n(b, y\prime)$ is the galaxy density calculated using

$$n(b,\,y') = \langle n\rangle\left[1 + \xi_{\rm m}(b,\,y')\right]. \tag{7}$$

Table 1. Number of Mg II doublet hits in the S:WS sample (second column) for different ranges of impact parameter to the cluster centre (indicated in the first column). The third column contains the number of hits corrected from the contribution from the field; the fourth column includes the effects of clustering for the correction and the fifth column shows the total number of QSO–cluster pairs.

Range in b/h_{71}^{-1} Mpc	$N_{\rm hits}$	Field corrected	Clustering correction	Number of QSO–cluster pairs
0.0–0.5	8	4.79	4.22	11
0.5–1.0	5	2.41	2.05	12
1.0–1.5	1	0.47	0.37	13
1.5–2.0	1	0.48	0.40	10

Table 2. Number of Mg II doublet hits in the S:St sample. Columns are as in Table 1.

Range in b/h_{71}^{-1} Mpc	$N_{\rm hits}$	Field corrected	Clustering correction	Number of QSO–cluster pairs
0.0–0.5	1	0.96	0.95	14
0.5–1.0	7	6.73	6.70	32
1.0–1.5	2	1.92	1.91	55
1.5–2.0	1	0.95	0.94	66

In the last expression, $\xi_{\rm m}(b, y')$ is the cluster-mass cross-correlation function:

$$\xi_{\rm m}(x, y') = \xi_{\rm m}(\sqrt{x^2 + y'^2}) = \xi_{\rm m}(r) = \beta \left(\frac{r}{r_0}\right)^{\gamma}, \quad (8)$$

where $r_0 = 5\,h^{-1}$ Mpc and $\gamma = -1.8$ parametrize the correlation function of the mass (see e.g. Padilla et al. 2004), and $\beta = 1.6$ represents the bias factor of haloes with the same median mass as our sample of RCS clusters (note the change of notation for the bias with respect to previous works), obtained using the 'concordance cosmology' and the Sheth, Mo & Tormen (2001) formalism. As we use the cross-correlation function between clusters and the mass, there is only one factor of the bias parameter instead of the square of the bias as it would be the case in the cluster autocorrelation function.

The effect of these two corrections can be appreciated in the number of absorption systems associated with clusters, for different ranges of impact parameter with respect to the cluster centre shown in Tables 1 and 2. Note that the effect of the corrections is very small for S:St, reinforcing the results from Paper I where the frequency of strong absorption systems in clusters of galaxies was found to be significantly larger than in the field.

3 MODELS

We use theoretical predictions from numerical simulations to estimate the median size of the cold-warm gas halo from the available statistics on Mg II absorption systems from cluster galaxies in the LOS of QSOs.

In order to do this, we use two different methods. One consisting a Monte Carlo simulation and another the analysis of the output of a semi-analytic model by Bower et al. (2006). The reason behind this choice is to allow our results to include a variance from the intrinsic assumptions present in very different modelling procedures, to allow a quantification of possible model-dependent effects. As mentioned above, both models adopt the 'concordance' cosmology. In the following subsections, we first present general definitions and notation, and then show the details of each of the models.

3.1 Notation and definitions

In the models we will make reference to two distinct types of objects: (i) cluster-mass dark matter haloes and (ii) galaxies residing within these clusters. In all cases, the impact parameter will refer to the projected distance in physical units at the comoving distance to the cluster between the QSO LOS and the centre of the cluster (real or simulated); we will use the notation b for this impact parameter. In the case of individual galaxies, we will refer to two separate quantities: (i) the scalelength of the gaseous disc, $r_{\rm disc}$, and (ii) the extent of the Mg II halo capable of producing a Mg II absorption feature above a minimum EW, W_0^{2796}, that will be accordingly specified. The Mg II halo in the model galaxies is assumed to be a uniform cloud of constant density with no holes (filling factor of unity; see Section 5.2 for a discussion of the effects of a different value). Finally, in all cases, the observational sample to be compared with the models will be characterized by its median EW.

3.2 Halo occupation Monte Carlo simulations

The HO model is used in the literature to test whether the properties of individual galaxies depend on their host halo mass (e.g. Cooray 2005); its parameters can be adjusted using observed galaxy properties such as their clustering (see e.g. Zehavi et al. 2004) and luminosity functions in different bands (Cooray 2006). A HO model does not include physical prescriptions for galaxy evolution, although it can be used to infer the evolution of the population of galaxies in haloes via comparison with observations at various redshifts.

In this first approach, we use a HO model with parameters adjusted by Cooray (2006) to match the luminosity function of Sloan Digital Sky Survey (Abazajian et al. 2005) galaxies brighter than r band absolute magnitudes $M_r = -17$. This HO model assumes that the number of galaxies per halo depends on the halo mass such that haloes with masses above a minimum value $M_{\rm min} = 2.8 \times 10^{10}\,h_{71}^{-1}\,{\rm M}_{\odot}$ host one central galaxy, and the number of satellite galaxies per halo increases according to a power law $N_{\rm sat} = (M/M_{\rm sat})^{\beta}$, where M is the dark matter mass of the host halo, $M_{\rm sat} = 1.69^{+3.2}_{-1.5} \times 10^{13}\,h_{71}^{-1}\,{\rm M}_{\odot}$ and $\beta = 0.76 \pm 0.18$.

We combine this recipe with a projected Navarro, Frenk & White (1997, hereafter NFW) profile (from Yang et al. 2003) which we assume is followed by galaxies populating dark matter haloes. The NFW profile allows us to determine the projected density of galaxies as a function of the distance to the cluster centre, which is scaled according to the expected number of galaxies for clusters of a given mass, obtained from the HO model. The projection of the NFW profile is done by integrating the three-dimensional profile on the direction of the LOS out to two virial radii from the cluster centre (see Yang et al. 2003, for more details). We use this projected galaxy number density, $\sigma(b)$, as a function of the projected distance to the cluster centre to determine the median Mg II halo size, $r_{\rm Mg\,II}$, necessary to produce a given frequency of hits, $N_{\rm hits}/N_{\rm LOS}$, in a sample of $N_{\rm LOS}$ QSO–cluster pairs using

$$r_{\rm Mg\,II} = \sqrt{\frac{N_{\rm hits}}{\pi\,\sigma(b) N_{\rm LOS}}}, \quad (9)$$

where we have assumed that all galaxies have equal Mg II halo sizes.

Fig. 1 shows the expected number of hits per QSO–cluster pairs for clusters with median masses of $10^{13.8}\,h_{71}^{-1}\,{\rm M}_{\odot}$ (top panels), increasing to $10^{15.3}\,h_{71}^{-1}\,{\rm M}_{\odot}$ (bottom panels). We show the results for 1, 2 and 3 simultaneous hits (solid, dashed and dotted lines) in the LOS of one target quasar as a function of the median impact parameter, $b_{\rm m}$, calculated at the median redshift of the RCS cluster sample, median $(z) = 0.6$. In this case, we assume two values for the median Mg II halo sizes, $r_{\rm Mg\,II} = 50$ and $80\,h_{71}^{-1}$ kpc (left- and right-hand panels, respectively), which correspond to a range of sizes consistent with estimates from absorption systems of field galaxies in QSO spectra (Churchill 2001; Churchill & Vogt 2001; Nestor et al. 2005). The models show that it is easier to obtain more events of multiple hits when observing more massive clusters as well as when choosing background QSOs closer to the cluster centres. Also, a larger Mg II halo will produce more hits, as expected. These plots allow us to study the particular case of LOS number 14 from Paper I, where two Mg II absorption systems overlap with the allowed ranges of photometric redshifts of six individual RCS clusters. Using the expected frequency for single and double hits for the median mass of our RCS cluster sample, the resulting likelihood that both Mg II systems correspond to only one out of the six clusters is $\simeq 10^4$ times lower than the case where the individual absorptions are associated with two different clusters (out of the available six). This calculation corresponds to the average impact parameter $b_{\rm m} = 1200\,h_{71}^{-1}$ kpc, characterizing this LOS, and considers the measured median masses of the RCS clusters in our sample (in the case where the double and single hits are equally likely, the former are only $\simeq 5$ times less likely

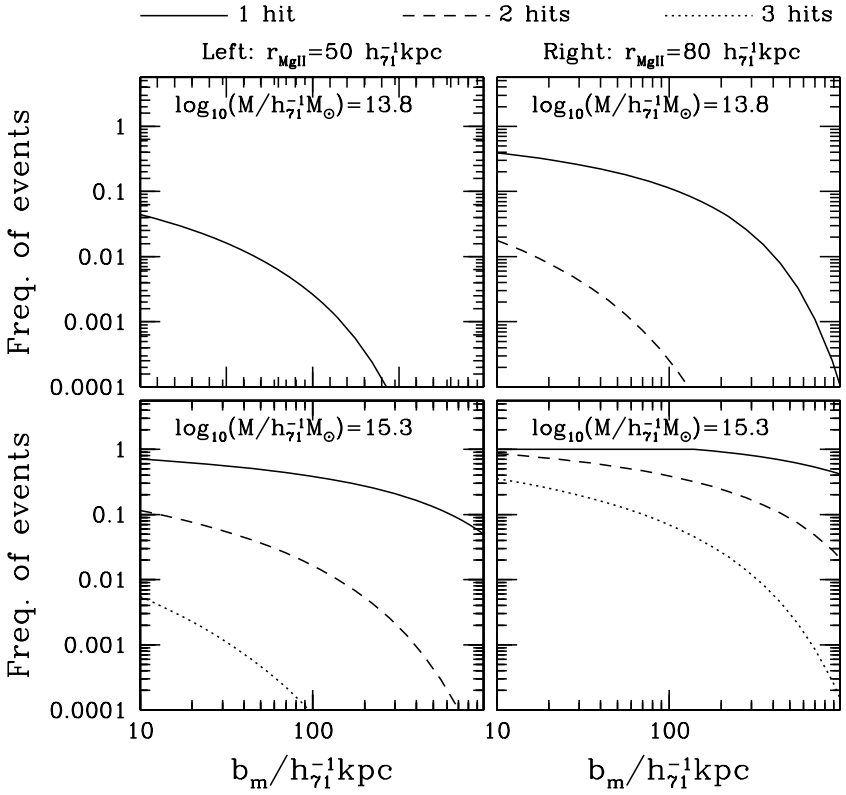

Figure 1. HO model: number of events relative to the number of QSO–cluster pairs of single, double and triple hits (solid, dashed and dotted lines, respectively) as a function of median impact parameter measured with respect to the cluster centre. Left- and right-hand panels show the results from considering $r_{\rm gal} = 50$ and $80\,h_{71}^{-1}$ kpc, respectively. The cluster mass increases from the top to the bottom panels as indicated in the key.

to happen than the latter for this LOS). Therefore, from this point on, we consider this case as two single hits (Table 1 is constructed accordingly). This would not be the case if the multiple absorption system was consistent with the photometric redshift of a single RCS cluster. This particular LOS offers an excellent laboratory for follow-up spectroscopy of absorbers.

We estimate the relative errors in Mg II halo sizes, $\Delta r_{\rm Mg\,II}/r_{\rm Mg\,II}$, assuming Poisson statistics and using the frequency of single hits and samples of different total number of QSO–cluster pairs. For this calculation, we adopt fixed values of cluster mass, $M = 1.64 \times 10^{14}\,h_{71}^{-1}\,{\rm M}_{\odot}$, and impact parameter, $b = 1339\,h_{71}^{-1}$ kpc, corresponding to the median values in our full sample of QSO–RCS cluster pairs. In Fig. 2, we show the variation of $\Delta r_{\rm Mg\,II}/r_{\rm Mg\,II}$ for three different Mg II halo sizes as a function of the number of QSO–cluster pairs. The vertical grey line indicates the expected errors in the Mg II halo size for the total number of 529 pairs in sample S:St, and indicates that for sizes larger than $\simeq 50\,h_{71}^{-1}$ kpc, the uncertainties would be below 25 per cent of the inferred size.

We will use this model to infer the typical size of the Mg II halo and its associated measurement error in the observational data described above.

In what follows, we introduce the details of the additional model which uses a cosmological numerical simulation in combination with a semi-analytic model of galaxy formation.

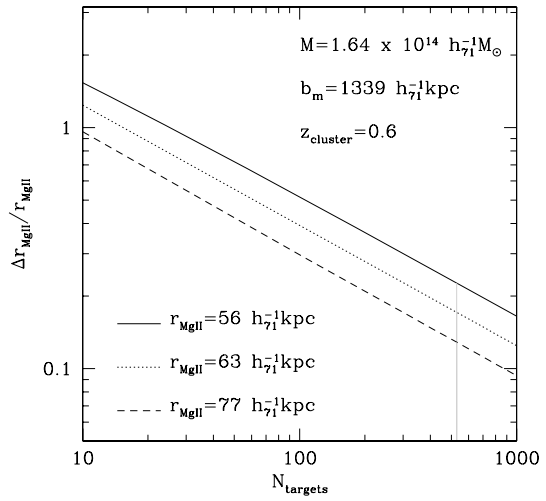

Figure 2. HO Model: relative errors in $r_{\rm Mg\,II}$ as a function of number of target QSOs for a fixed cluster mass of $M = 1.64 \times 10^{14}\,h_{71}^{-1}\,{\rm M}_{\odot}$ and median impact parameter $b_{\rm m} = 1339\,h_{71}^{-1}$ kpc. Results are shown for $r_{\rm Mg\,II} = 56$, 63 and $77\,h_{71}^{-1}$ kpc. The grey vertical line shows the number of QSO–cluster pairs in the S:St sample.

3.3 GALFORM semi-analytic galaxies

This model differs from the HO in that it follows the evolution of galaxies using a number of physical prescriptions for the different galaxy components, including cold gas, stars, metallicity of stars and gas (hot and cold), and the properties of the central supermassive black hole. However, there is a strong observational component to the model since its parameters are tuned to match the observed galaxy population at various redshifts.

The main advantage in using a semi-analytic model relies on the following. The global properties of large concentrations of matter in either simulations or observations are well known on average; however, the complex nature of the non-linear collapse that formed virialized objects has important consequences on their diversity, even for objects of similar masses. The properties that are not included in a general description of clusters include their asphericity, substructure and formation history, and their relation to the surrounding environment. Therefore, the use of a cosmological numerical simulation allows us to include this diversity in the population of cluster-size dark matter haloes, an effect that is very difficult to include in the model presented in the previous subsection, which relies on Monte Carlo modelling.

In this work, we use the Bower et al. (2006) GALFORM galaxy catalogue which conforms a complete sample of galaxies down to a magnitude $M_r = -17$. These galaxies populate the Millennium Simulation (Springel et al. 2005), which follows the evolution of $\simeq 1 \times 10^{10}$ collisionless dark matter particles from $z = 50$ to the present on a box of $704.2\,h_{71}^{-1}$ Mpc a side, for a mass resolution per particle of $1.21 \times 10^9\,h_{71}^{-1}\,\mathrm{M}_\odot$. This simulation allows us to identify bound dark matter structures and follow their descendants at different redshifts. This, in turn, can be used to infer the galaxy population within each dark matter halo, via various assumptions regarding the different processes that shape the formation and evolution of galaxies in a semi-analytic model (De Lucia et al. 2006; Croton, Gao & White 2007; Malbon et al. 2007; Lagos, Cora & Padilla 2008).

It is important to note that these galaxies do not include a description of their Mg II content, and therefore can only be used in a similar way to the HO model procedure. Given that the model follows the evolution of the disc scalelength, $r_{\rm disc}$ of each individual galaxy with time, we assume that the radius of the Mg II haloes will be

$$r_{\rm Mg\,II} = A \times r_{\rm disc}, \tag{10}$$

where A is a proportionality constant that will be varied in order to match the observed frequency of Mg II absorption events. This is an important hypothesis that we will adopt throughout this work, namely, that the size of the Mg II halo is proportional to the disc size.

Our sample of simulated clusters is constructed by selecting all systems above a minimum mass such that the median mass equals that present in our RCS cluster sample.

3.3.1 Simulated composite cluster

In order to study the frequency of galaxies in front of background QSOs in the numerical model, we construct a composite cluster using all the objects within our sample of simulated clusters. We do this by stacking all the clusters using their most bound particle as their centres; the semi-analytic model by Bower et al. (2006) uses this position to place the central galaxy of each halo. The stacking procedure erases all cluster membership information. Therefore, our simulated composite cluster cannot be used to study multiple absorption events from individual clusters. As was mentioned above, the multiple hit candidate present in the data from Paper I is considered as two single hits due to its low probability of occurrence.

Given that the population of background QSOs is at a very large distance behind the clusters in our sample, we assume that the former are distributed at random within $2\,h_{71}^{-1}$ Mpc from the cluster centres, in projection.

3.3.2 Morphological types

Among the information available for each galaxy in the semi-analytic model are the stellar mass in the disc and bulge components. Therefore, it is possible to separate a population of elliptical and spiral galaxies, which may prove important in light of previous results suggesting the presence of strong Mg II absorption systems mainly in spiral systems (Zibetti et al. 2007).

Therefore, our analysis of number of galaxies in the LOS of background QSOs is done to a first approximation only on spiral galaxies selected so that the stellar content in their bulges is only up to 70 per cent of the total stellar mass (Bertone, De Lucia & Thomas 2007).[4]

We bear in mind that Zibetti et al. (2007) also show that there may be dependencies of the Mg II absorption on galaxy colour and morphology. Given the simplicity of the approach we follow in this work, we will not attempt to model this dependency but instead will offer estimates on the expected impact of the morphological selection on our results in Section 5.2.

4 RESULTS

In this section, we provide separately the results obtained using the two models presented in the previous section, first from the observationally motivated HO model, and secondly from the semi-analytic model galaxies in the Millennium Simulation (Springel et al. 2005).

4.1 HO model

We use equation (9) to determine the sizes of galaxy Mg II haloes that would produce the rate of hits shown in Table 1 (only calculated for the S:WS sample), for clusters with median mass $1.64 \times 10^{14}\,h_{71}^{-1}\,\mathrm{M}_\odot$. We show the resulting typical sizes in Fig. 3 for the total number of hits in the S:WS sample (open squares) and also for the corrected counts by the expected contamination from the field (open pentagons) and clustering (open triangles). The results when considering the 'farthest cluster' variant of our S:WS sample fall within the error bars of these estimates, and therefore are not shown. Error bars are calculated by assuming Poisson statistics. The points along the abscissa correspond to the middle of the bin in b, with small shifts for the different cases, added to improve clarity.

An important change in the inferred Mg II halo sizes is produced when one of the cluster members is placed at the centre of the cluster (i.e. a central galaxy). This affects the innermost region for which it is straightforward to infer the expected fraction of LOS that would pass through the central galaxy Mg II halo once its typical size, $r_{\rm Mg\,II}$, is known. This is an iterative process which converges rapidly after three iterations. When taking this into account, the results change quite dramatically for the low-impact parameter bin as it is shown by the open star symbols in Fig. 3. These results indicate that near the cluster centres, the Mg II halo of a galaxy could either be as large as $r_{\rm Mg\,II} \simeq 16\,h_{71}^{-1}$ kpc or as small as $r_{\rm Mg\,II} \simeq 2\,h_{71}^{-1}$ kpc, depending on whether a central galaxy is assumed to lie exactly at the observationally determined cluster centre (which is subject to uncertainties).

[4] Bertone et al. find that in the case of the semi-analytic model we are using in this work, a limit of 70 per cent of the total mass in stars is the minimum fraction for early-type objects that allow us to reproduce the observed dependence of morphological fractions as a function of stellar mass and local density.

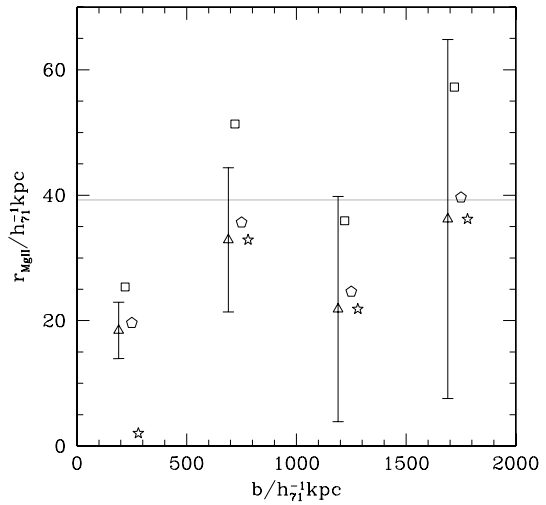

Figure 3. HO Model: Mg II halo sizes as a function of impact parameter, according to the HO model results. Open squares show the results for the total number of hits in the S:WS sample, open pentagons correspond to the number of hits corrected by the expected field hits and open triangles show the results from adding the correction for clustering. The open star symbols indicate the resulting sizes when one of the cluster members is positioned at the centre of mass of the cluster. The horizontal solid line indicates the radius of Mg II haloes in the field obtained from the HO model.

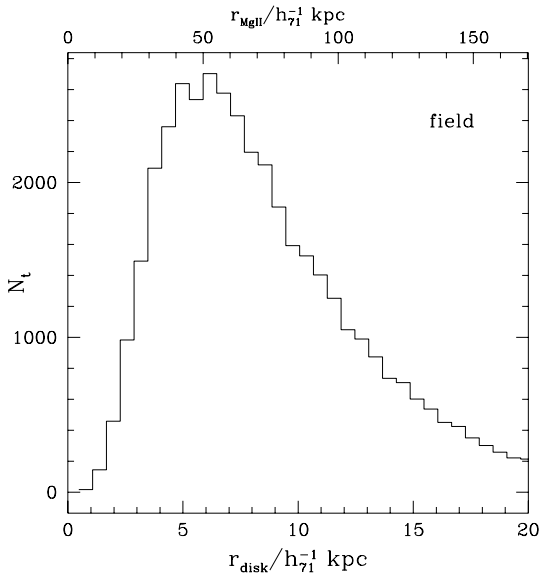

Figure 4. Semi-analytic model: histogram of galaxy disc scalelengths (lower x-axis) and Mg II galaxy haloes (upper x-axis) needed to reproduce the number of hits reported for the field.

Our results show that the typical size of the Mg II halo tends to increase towards the outskirts of the cluster. This result is independent of the corrections applied to the observational data, and not sensitive to the presence of a central galaxy at the centre of mass of the cluster. This is also in reasonable agreement with previous studies that report that the cold/cold-warm gas haloes around galaxies may be stripped off by the hot intracluster gas (see e.g. Heinz et al. 2003).

We also use the HO model to estimate the typical Mg II halo size in the field, which is indicated by the horizontal grey solid line in Fig. 3. We estimate this size by integrating over the full range of halo masses where dark matter haloes are expected to have at least one galaxy with $M_r < -17$, for the EW range corresponding to sample S:WS. As can be seen, our estimate of $r_{\rm Mg\,II} \simeq 39\,h_{71}^{-1}$ kpc (in broad agreement with observational estimates, e.g. Churchill et al. 1999) is slightly larger than our findings for the inner cluster environment, in agreement with the stripping scenario in clusters. For reference, the galaxy number density in the HO model is $n = 7.639 \times 10^{-3}/h_{71}^{-3}\,{\rm Mpc}^3$. Note that this result corresponds to the HO model; the results from the analysis of the semi-analytic model for the field are presented in the following subsection.

4.2 GALFORM semi-analytic model

Given the better description of individual clusters allowed by the combination of a numerical simulation and a semi-analytic model, the results from the composite cluster may provide further clues regarding the dependence of Mg II halo on the distance to the cluster centre.

We start by studying the expected typical halo size in the field. In order to do this, we randomly select positions in the simulation and take all the galaxies within $2\,h_{71}^{-1}$ Mpc in projection from these centres stacked together. This stack is characterized by a comoving length which we convert to a redshift path. We then place one QSO in the background and sort all the galaxies in the stack with respect to their projected distance to the QSO, and assume that their Mg II halo sizes will be directly proportional to their disc scalelengths, as was mentioned in Section 3.3. All the Mg II haloes defined this way that contain the LOS to the QSO are counted. We then vary the constant A until the simulation reproduces the same counts per unit redshift path, dN/dz, reported by the study of the field by Churchill et al. (1999)

Fig. 4 shows the results of the semi-analytic approach. It depicts the distribution of disc scalelengths in the field (lower x-axis label), where galaxies show a wide range of values with a peak at $r_{\rm disc} = 6\,h_{71}^{-1}$ kpc. The top x-axis label shows the resulting Mg II halo sizes, with a distribution peak at a value of $r_{\rm Mg\,II} \simeq 50\,h_{71}^{-1}$ kpc, well in agreement with the observational estimate of Churchill et al. (1999) for EW > 0.02 Å. Also note that our estimate from this approach is only slightly higher than the results from the HO presented in the previous section. This difference arises from the different EW limits assumed in each case (otherwise both results agree with each other).

The analysis of the composite cluster constructed from the GALFORM model also provides useful insights on the size of the Mg II haloes in the cluster environment, and particularly as a function of distance to the cluster centre. In the semi-analytic model, galaxy disc scalelengths show smaller typical sizes near the cluster centres as can be seen in Fig. 5, where we show the median size of galaxy discs (points; error bars indicate the error of the mean assuming Poisson statistics). This is a first indication that the model indeed includes important environmental effects on the galaxy population (note that these values are not to be compared to the field Mg II region sizes denoted as $r_{\rm Mg\,II}$). In the GALFORM semi-analytic model, the physical process driving the environmental changes within clusters is the removal of the hot gas reservoir around galaxies once they enter a new dark matter halo; this process effectively stops the cooling of gas on to the galactic disc halting its growth.

Following the procedure used to infer the typical sizes of Mg II haloes in the field, we also find the proportionality constant that multiplied by the disc scalelengths gives a Mg II cloud size that

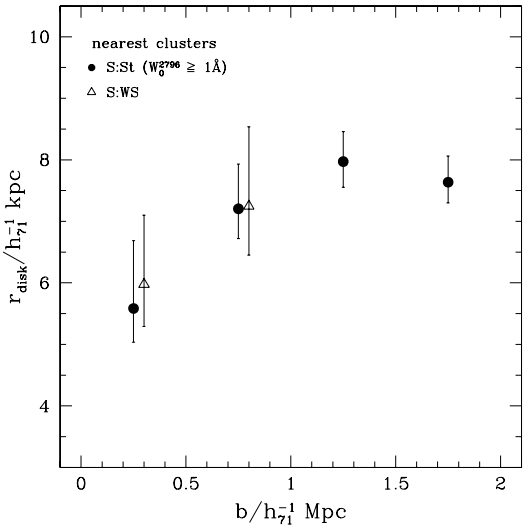

Figure 5. Semi-analytic model: dependence on impact parameter to the cluster centre of the median disc scalelength in the semi-analytic model. The error bars show the error of the median.

provides a match to the abundance of Mg II absorption systems in cluster–QSO pairs in the S:WS and S:St samples. Fig. 6 shows histograms of galaxy disc scalelengths (lower x-axes) and resulting typical Mg II halo sizes (top x-axes) for two ranges of impact parameter (increasing values of b from the left- to the right-hand panels) for the S:WS (top panel) and S:St (bottom panel) samples. The size distributions show a marked raise towards a single peak (on the position of these peaks we will centre our discussion) and a slower fall-off for higher values of $r_{\rm disc}$, with a distribution width that clearly increases towards the cluster outskirts, in both disc and Mg II halo sizes. From the location of the peaks, it can be seen that the increase in the disc scalelengths with the impact parameter shown in Fig. 5 is confirmed. It can also be seen that the location of the Mg II size distribution peaks shows a similar trend of larger values further away from the cluster centres. Furthermore, the Mg II halo sizes are consistent with larger values for the S:WS sample for the lowest impact parameter bin, which reflects the fact that the frequency of Mg II absorption events is higher in this sample than in S:St at such distances from the cluster centre.

Fig. 7 shows the median size of a Mg II cloud as a function of the distance to the cluster centre (error bars show the error of the median) for the S:WS (triangles) and S:St (circles) samples. As can be seen from both figures, the trend of a larger galaxy size at larger distances from the cluster centre is clearly found in both samples with values ranging from $r_{\rm Mg\,II} \simeq 2$–$6\,h_{71}^{-1}$ kpc at $b < 0.5\,h_{71}^{-1}$ Mpc to $r_{\rm Mg\,II} \simeq 25\,h_{71}^{-1}$ kpc at $b > 1.5\,h_{71}^{-1}$ Mpc, in good agreement with the HO results with a central galaxy.[5] The corresponding inferred size for typical Mg II haloes in the field for the range of EW in sample S:WS for the semi-analytic model is $40\,h_{71}^{-1}$ kpc (note that this value differs slightly with the result from Fig. 4, due to the different EWs considered).

We remind the reader that these results are motivated by the observational frequency of Mg II absorption systems in our samples of RCS cluster–QSO pairs (the proportionality constant in equation 10 depends on the impact parameter). Therefore, the trends of smaller Mg II halo (cf. Fig. 7) and disc sizes (cf. Fig. 5) towards the cluster centres are independent results. Furthermore, the reasonable consistency between the results from the HO model and the semi-analytic simulation provides further reliability to the findings on the trends of Mg II halo size with the distance to the cluster centre.

[5] Note that the Mg II halo size at $b > 1.5\,h_{71}^{-1}$ Mpc is not expected to resemble the Mg II halo size inferred for the field since this sample contains only galaxies in high-mass dark matter haloes, and therefore does not include a representative sample of field galaxies, even in the cluster outskirts.

5 DISCUSSION

In the previous section, we studied the inferred typical Mg II halo sizes using two different models, the HO and the output from a semi-analytic simulation. We find that both models are able to reproduce the observed frequency of Mg II absorption events found in observational data in Paper I. More importantly, our results indicate that the Mg II halo sizes tend to increase from relatively low values of $r_{\rm Mg\,II} \simeq 2$–6 to 26–$40\,h_{71}^{-1}$ kpc for $b = 0.5\,h_{71}^{-1}$ Mpc to $b > 1.5\,h_{71}^{-1}$ Mpc; both models produce consistent results.

In what follows, we present a study of the fraction of the Mg II halo responsible for producing different Mg II absorption-line strengths, and an analysis of possible systematic effects present in our current measurements.

5.1 Regions of strong Mg II absorption-line systems

We take full advantage of the additional information available in the semi-analytic model regarding the galaxy disc scalelengths, and combine this with previous results by Chen & Tinker (2008) who find that stronger absorption systems are produced by clouds closer to the galaxy centres[6] to study the typical size of the regions in the Mg II halo responsible for different absorption-line strengths.

In our analysis of the semi-analytic model, we maintain a record of the distance, d, between each QSO LOS and each galaxy centre. Therefore, after finding the proportionality constant A (equation 10) that reproduces the frequency of hits found in Paper I, we can sort the galaxies with respect to d. Then, for different ranges of cluster-centric impact parameter, we study the observed fractions of different line strengths, and find the galactocentric distance out to which the same fractions of model galaxies are included. Such a distance is then identified as the maximum distance out to which a given line strength would be produced in the model. Fig. 8 presents the resulting fraction of the Mg II halo size out to which a given line strength occurs, as a function of distance to the cluster centre. This rescaling is adopted in order to factor out the measured variation of the global Mg II halo size with the impact parameter to the cluster centre. Open and solid symbols represent high ($W_0^{2796} > 2$ Å) and low ($W_0^{2796} < 2$ Å) EW absorption systems, respectively; triangles correspond to results from the S:WS sample, circles to S:St. In the case of the high EW results, the large error bars only allow a possible rejection of an increase in the Mg II halo region producing such absorption events. However, there is a mild indication that the low EW absorption systems (all from S:WS) tend to occur at increasingly larger distances from the galaxy centre in terms of the Mg II halo size towards the outskirts of clusters. These results are again in good agreement with the stripping scenario, where the low-density Mg II clouds within a given galaxy would be more easily removed than the denser Mg II regions nearer the galaxy centre that would be responsible for high EW absorption systems.

[6] In their terminology, this would be a halo centre, which can be applied to each galaxy in the semi-analytic model since these are located at the centres of bound substructures (or subhaloes) in the numerical simulation.

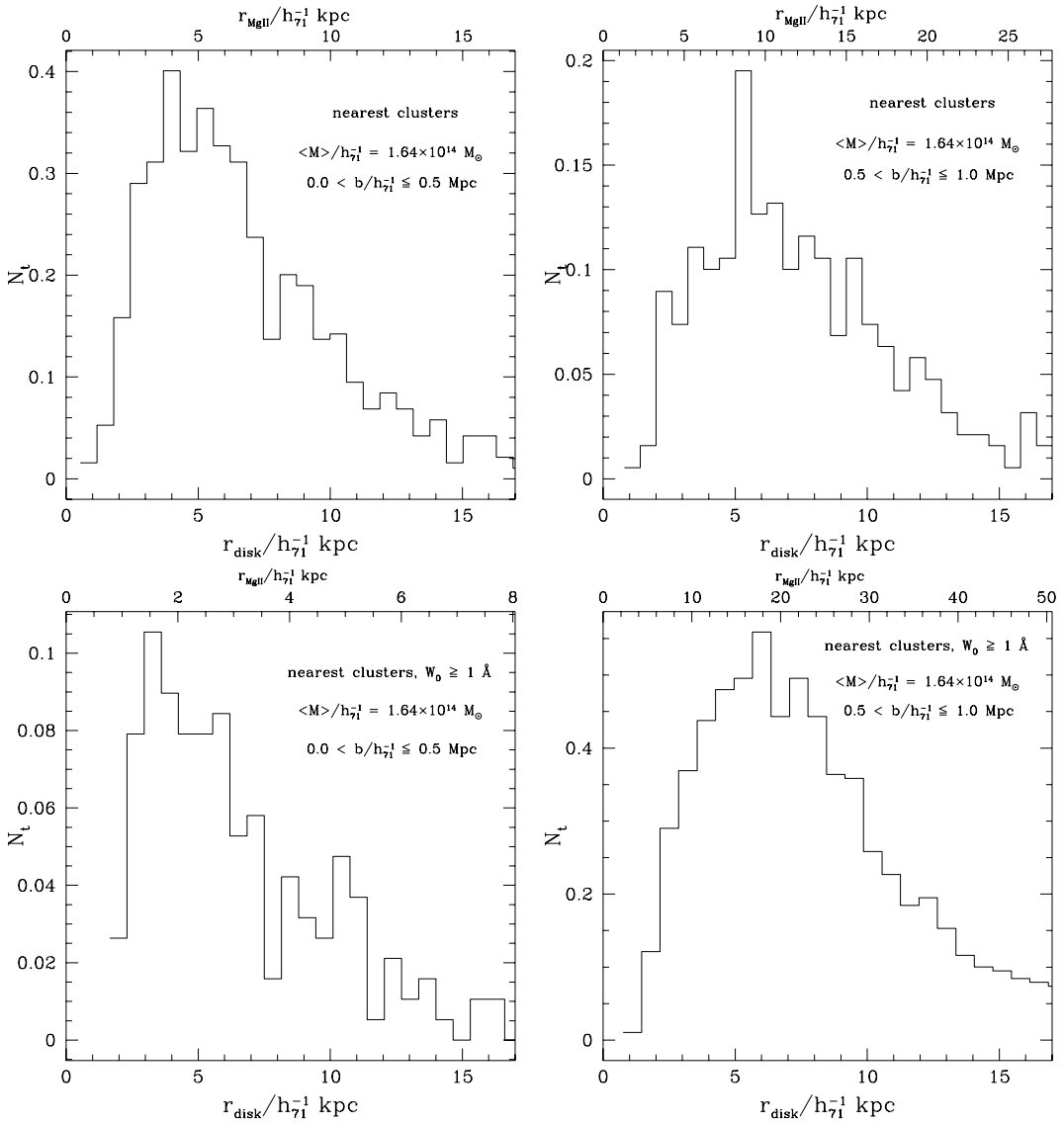

Figure 6. Semi-analytic model: histogram of galaxy disc scalelengths (lower *x*-axes) and Mg II galaxy haloes (upper *x*-axes) needed to reproduce the number of hits in the observations, for different ranges of impact parameter *b*, shown in the key (increasing values from left- to right-hand panels) for the S:WS and S:St samples (top and bottom panels, respectively).

5.2 Possible systematic effects

The parametrization of both models, HO and semi-analytic, used to mimic the observational procedure carried out in Paper I, depends on a number of parameters, assumptions and measurements that can induce systematic effects.

For instance, the results shown in the previous sections were obtained for clusters of a median mass corresponding to the estimates for the RCS clusters. In order to assess the possible systematic biases arising from errors in these cluster mass measurements, we change the adopted median mass by factors of 4 and 0.25, approximately 0.6 dex in the cluster mass. The results in the HO and semi-analytic models are affected by very similar relative variations, which do not show a dependence with the distance to the cluster centre. When the lower value for the median mass is adopted, the inferred median sizes of the Mg II haloes increase by ∼10 per cent; alternatively, a higher median mass produces a decrease in the inferred size by a 20–25 per cent. Given that the effect does not vary with the distance to the cluster centre, our conclusions would not be significantly affected by this source of systematic uncertainties.

It should also be taken into account that in our modelling, we have considered spherical Mg II haloes. Given the lack of detailed information on the thickness of cold gas discs, we do not venture into assuming a given disc thickness in this work, as has also not been done in previous works studying the size of Mg II absorption regions in the field as in Churchill et al. (1999).

It has been argued that a unity covering fraction for Mg II haloes is rather unlikely (Bechtold & Ellingson 1992; Tripp & Bowen 2005; Chen & Tinker 2008; Kacprzak et al. 2008). Since the models we have adopted here assume a fixed value for the covering fraction (which we have chosen to be $C = 1$), we cannot study a possible dependence with environment. However, it is easy to see that a different covering fraction will change our results on the Mg II halo sizes according to $r_{\rm Mg\,II}$ to $r^C_{\rm Mg\,II} = \frac{1}{\sqrt{C}} r_{\rm Mg\,II}$.

Finally, the effect from considering absorption from low-gas content galaxies should also be taken into account. In the semi-analytic

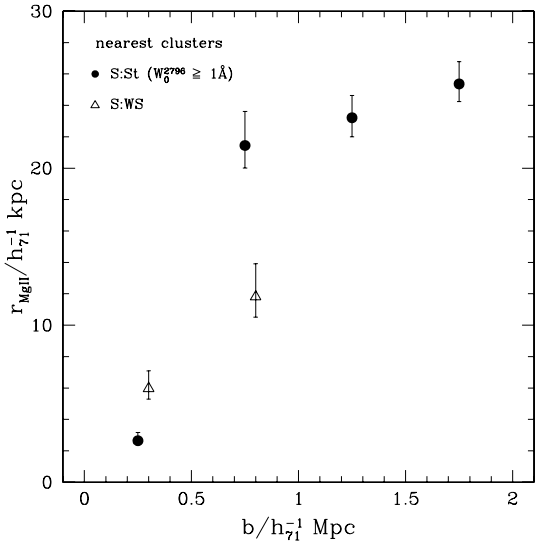

Figure 7. Semi-analytic model: median sizes of Mg II haloes as a function of projected distance to the cluster centre. Error bars show the error of the median.

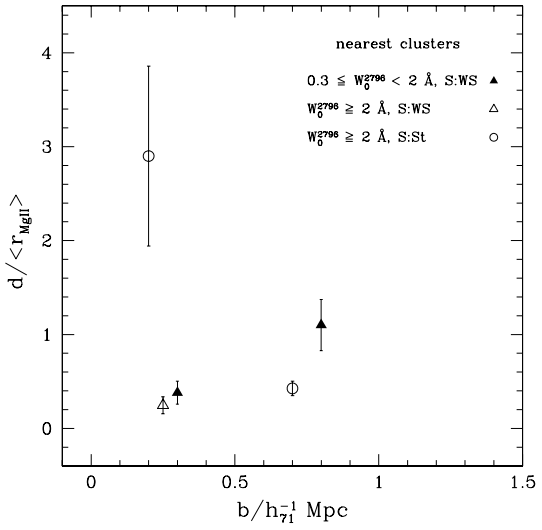

Figure 8. Semi-analytic model: extent of different absorption-line EWs in units of the Mg II halo radius, as a function of impact parameter to the cluster centres. The results from the S:WS sample are shown by triangles, and from the S:St sample are shown by circles. Open symbols correspond to strong absorption-line systems and filled symbols correspond to weak absorption lines.

model, the fraction of elliptical galaxies changes as a function of the distance to the cluster centre. This is specially true for $r/r_{\rm vir} < 1$, where the fraction of model elliptical galaxies (see Section 3.3.2) increases from $\sim$15 per cent to $\sim$50 per cent at $r/r_{\rm vir} = 0.015$, measured in projection [these fractions are in good agreement with results from the Sloan Digital Sky Survey (SDSS) from Goto et al. 2003]. At larger distances from the cluster centres, the fraction of elliptical galaxies remains practically unchanged. For sample S:WS (and similarly for sample S:St), considering an absorption from elliptical galaxies in the semi-analytic model would increase by a factor of $\sim$1.43([7]) the number of potential absorbers and therefore decrease our estimate of the typical Mg II size inside clusters by a 16.4 per cent. Our estimates at larger distances from the cluster centre will be equally affected by a decrease of approximately 7.8 per cent. The latter estimate would also change our estimates for the typical Mg II halo size inferred for the field accordingly in both, the semi-analytic and HO models. In consequence, our conclusions do not change significantly due to this effect.

6 SUMMARY AND CONCLUSIONS

In this paper, we have presented a theoretical study of Mg II halo sizes of galaxies in clusters and the field, by comparing recent observational results on the incidence of Mg II absorption systems in RCS cluster–QSO pairs by Paper I, and the predicted systems from the HO and semi-analytic models.

As a first step in our analysis, we applied corrections to the observed frequency of absorption events to take into account possible contaminations from the field, and effects of the Large–Scale Structure.

The results from the HO and semi-analytic models indicate that the typical field Mg II halo is $r_{\rm gal} \simeq 39$–$50\,h_{71}^{-1}$ kpc (for EW > 0.02 Å), a value in broad agreement with previous results pointing towards $r_{\rm gal} \simeq 50$–$100\,h_{71}^{-1}$ kpc found for similar absorber EWs (Churchill et al. 2001; Zibetti et al. 2007; Chen & Tinker 2008; Kacprzak et al. 2008).

The HO model also indicates that the Mg II halo tends to be smaller near the cluster centres, reaching values of $r_{\rm gal} \simeq 16\,h_{71}^{-1}$ kpc. When one of the cluster members occupies the centre of mass of the cluster, the Mg II halo size can be as low as $\simeq 2\,h_{71}^{-1}$ kpc. This result is obtained assuming a fixed galaxy size for all the cluster members. The results from the semi-analytic model are consistent with those from the HO showing a clear decrement in the typical Mg II size towards the cluster centres. An interesting by-product of this analysis is that the galaxy disc scalelengths in the model also show a clear increase towards the outskirts of clusters, in accordance with the scenario where strong interactions strip galaxies of their outer discs in cluster environments.

We also used the semi-analytic model to estimate the radii of Mg II haloes producing different strengths of absorption. In order to do this, we assumed that stronger lines are produced nearer the centres of galaxies (following Chen & Tinker 2008). We found that in terms of the Mg II halo size, the strong absorption regions occur out to a rather fixed value, independent of the distance to the cluster centre. However, weaker absorption-line systems show a tendency to occur at larger distances from the galaxy centre (in units of their global Mg II halo radius) towards the outskirts of clusters. This trend could explain the flatter EW distribution found in Paper I, that included all impact parameters within $b < 2\,h_{71}^{-1}$ Mpc.

Our results indicate that the effect of the cluster environment on galaxies is extremely important and can produce a decrement of up to a 90 per cent of the Mg II halo size with respect to galaxies in more gentle environments such as the field.

[7] This is an upper limit for the contribution of ellipticals to the projected galaxy number density at a median impact parameter of $b/r_{\rm vir} = 0.17$. This value corresponds to the first bin in our measurements of $r_{\rm Mg\,II}$, $b < 500\,h_{71}^{-1}$ kpc, for the median virial radius of the clusters, $r_{\rm vir} = 775\,h_{71}^{-1}$ kpc.

ACKNOWLEDGMENTS

SL, LFB, PL and NP were partly supported by the Chilean Centro de Astrofísica FONDAP No. 15010003. NDP was also supported by FONDECYT grant No 1071006, SL by FONDECYT grant No 1060823 and LFB by FONDECYT grant No 1085286. We thank the anonymous referee for helpful comments and suggestions. Funding for the SDSS and SDSS-II has been provided by the Alfred P. Sloan Foundation, the Participating Institutions, the National Science Foundation, the US Department of Energy, the National Aeronautics and Space Administration, the Japanese Monbukagakusho, the Max-Planck Society and the Higher Education Funding Council for England. The SDSS web site is http://www.sdss.org/.

REFERENCES

Abazajian K., The SDSS Team, et al., ApJ, 2005, 625, 613
Baugh C. M., Lacey C. G., Frenk C. S., Granato G. L., Silva L., Bressan A., Benson A. J., Cole S., 2005, MNRAS, 356, 1191
Bechtold J., Ellingson E., 1992, ApJ, 396, 20
Bergeron J., Stasinska G., 1986, A&A, 169, 1
Berlind A. A., Weinberg D. H., 2002, ApJ, 575, 587
Bertone S., De Lucia G., Thomas P. A., 2007, MNRAS, 379, 1143
Bouche N., Murphy M., Péroux C., Csabai I., Wild V., 2006, MNRAS, 371, 495
Bower R. G., Benson A. J., Malbon R., Helly J. C., Frenk C. S., Baugh C. M., Cole S., Lacey C. G., 2006, MNRAS, 370, 645
Chen H., Tinker J., 2008, ApJ, 687, 745
Churchill C., 2001, ApJ, 560, 92
Churchill C., Vogt S., 2001, AJ, 122, 679
Churchill C. W., Rigby J. R., Charlton J. C., Vogt S. S., 1999, ApJS, 120, 51
Churchill C. W., Mellon R. R., Charlton J. C., Jannuzi B. T., Kirhakos S., Steidel C. C., Schneider D. P., 2000, ApJ, 543, 577
Churchill C., Kacprzak G., Steidel C., 2005, in Williams P. R., Shu C.-G., Ménard B., eds, IAU Colloq. 199 Probing Galaxies Through Quasar Absorption Lines. Cambridge Univ. Press, Cambridge, p. 24
Cole S., Lacey C., Baugh C., Frenk C., 2000, MNRAS, 319, 168
Cooray A., 2005, MNRAS, 364, 303
Cooray A., 2006, MNRAS, 365, 842
Croft R. A. C., Dalton G. B., Efstathiou G., Sutherland W. J., Maddox S. J., 1997, MNRAS, 291, 305
Croton D. et al., 2006, MNRAS, 367, 864
Croton D., Gao L., White S. D. M., 2007, MNRAS, 374, 1303
De Lucia G., Springel V., White S. D. M., Croton D., Kauffmann G., 2006, MNRAS, 366, 499
Ellison S. L., Kewley L. J., Mallén-Ornelas G., 2005, MNRAS, 357, 354
Gilbank D., Yee H. K. C., Ellingson E., Gladders M. D., Barrientos L. F., Blindert K., 2007, AJ, 134, 282
Gladders M. D., Yee H. K. C., 2005, ApJS, 158, 161
Goto T., Yamauchi C., Fujita Y., Okamura S., Sekiguchi M., Smail I., Bernardi M., Gomez P., 2003, MNRAS, 346, 601
Heinz S., Churazov E., Forman W., Jones C., Briel U. G., 2003, MNRAS, 346, 13
Kacprzak G., Churchill C., Steidel C., Murphy M., 2008, AJ, 135, 922
Lagos C., Cora S., Padilla N., 2008, MNRAS, 388, 587
Lanzetta K. M., Turnshek D. A., Wolfe A. M., 1987, ApJ, 322, 739
Lopez S. et al., 2008, ApJ, 679, 1144 (Paper I)
Lynch R. S., Charlton J. C., Kim T. S., 2006, ApJ, 640, 81
Malbon R., Baugh C., Frenk C., Lacey C., 2007, MNRAS, 382, 1394
Navarro J., Frenk C., White S., 1997, ApJ, 490, 493 (NFW)
Narayanan A., Misawa T., Charlton J. C., Kim T., 2007, ApJ, 660, 1093
Nestor D. B., Turnshek D. A., Rao S. M., 2005, ApJ, 628, 637
Nestor D. B., Turnshek D. A., Rao S. M., 2006, ApJ, 643, 75
Padilla N., Merchán M., Valotto C., Lambas D. G., Maia M. A. G., 2001, ApJ, 554, 873
Padilla et al., The 2dFGRS Team, 2004, MNRAS, 352, 211
Petitjean P., Bergeron J., 1990, A&A, 231, 309
Prochter G. E., Prochaska J. X., Burles S. M., 2006, ApJ, 639, 766
Sánchez A., Baugh C. M., Percival W., Peacock J., Padilla N., Cole S., Frenk C., Norberg P., 2006, MNRAS, 366, 189
Scoccimarro R., Sheth R. K., Hui L., Jain B., 2001, ApJ, 546, 20
Sheth R. K., Mo H. J., Tormen G., 2001, MNRAS, 323, 1
Seljak U., 2000, MNRAS, 318, 203
Springel V. et al., 2005, Nat, 435, 629
Steidel C., Sargent W., 1992, ApJS, 80, 1
Steidel C., Bowen D., Blades I., Dickinson M., 1995, ApJ, 440, 45
Steidel C. C., Kollmeier J. A., Shapley A. E., Churchill C. W., Dickinson M., Pettini M., 2002, ApJ, 570, 526
Tinker J., Chen H., 2008, ApJ, 679, 1218
Tripp T., Bowen D., 2005, in Williams R. P., Shu C.-G., Menard B., eds, Proc. IAU Coll. Int. Astron. Union 199, Probing Galaxies through Quasar Absorption Lines, held March 14–18, Shanghai, People's Republic of China. Cambridge Univ. Press, Cambridge, p. 5
Tytler D., Boksenberg A., Sargent W., Young P., Kunth D., 1987, ApJS, 64, 667
Yang X., Mo H. J., Kauffmann G., Chu Y., 2003, MNRAS, 339, 387
Zehavi I. et al., 2004, ApJ, 608, 16
Zibetti S., Ménard B., Nestor D. B., Quider A. M., Rao S. M., Turnshek D. A., 2007, ApJ, 658, 161
Zheng Z., Weinberg D. H., 2007, ApJ, 659, 1

This paper has been typeset from a TEX/LATEX file prepared by the author.